Structure and evolution of the Carlsberg Ridge: Evidence for non-stationary spreading on old and modern spreading centres

S. A. Merkouriev* and N. A. Sotchevanova

SPbFIZMIRAN, Muchnov per, 2, Box 188, St. Petersburg, 191023, Russia

We present the results of magnetic and bathymetric data collected on board Russian vessels during the last decade. Our analysis shows that since late Cretaceous the proto-Carlsberg Ridge (CR) was spreading at a faster rate, prior to India's collision with Eurasia. Since Eocene, the present CR is characterized by slow spreading. Our results depict two discordant systems of linear magnetic anomalies. One corresponds with fast spreading with respect to latitude axis of the proto-ridge and the other with slow spreading with respect to modern axis of the CR, suggesting that the two spreading systems are asymmetric both relative to each other and relative to axial anomaly. We infer that during both these periods the structure and spreading on the CR was non-stationary.

THE Carlsberg Ridge (CR) extends from 2°S to 10°N, forming the NW–SE trending slow accreting plate boundary between the African and Indian Plates and continues as highly segmented Sheba Ridge in the Gulf of Aden to Red Sea[1,2] (Figure 1). In the region north of 10°N on the CR, the Arabia–India–Somalia triple junction has been evolving since last 16 m.y. as Ridge–Ridge–Ridge triple junction whose one arm trending N80°E is the ultra slow divergent boundary between Arabian and Indian Plate[3]. The evolution of the northern-western Indian Ocean (NWIO) is the last event of the break-up of Gondwana, when seafloor spreading progressively stopped in the Mascarene Basin[4]. India and Seychelles started separating along the Proto-CR[5–7]. The spreading rate was not constant and the phase of ultra-slow spreading (< 8 mm/a) between about A18 (40 Ma) and A7 (24 Ma) was detected[8]. CR on the modern phase is characterized by slow spreading and segmented by a few transforms and non-transform discontinuities[9–11]. The recent results[12] discussed the presence of an axial discontinuity at 3°32′N in terms of a propagating ridge head. The objective of the present study was to know the evolutionary history, the nature of spreading and structure of CR since the late Cretaceous.

Data acquisition and processing

Detailed bathymetric and magnetic survey of CR between 9°N–58°E and 2°S–69°E (Figure 1) was carried out mainly in the 1980s during successive Russian expeditions. The digitization and compilation of these datasets were completed during 1990s. All magnetic anomaly and bathymetric profile data were digitized, combined, totally reprocessed and loaded into the coherent magnetic and bathymetric database. The close spacing (5–6 km) between profiles allowed building accurate bathymetric and magnetic grids at a 2 min spacing for mapping in colour shaded relief and contours maps. The corresponding gravity dataset is obtained from the global FAA deduced from satellite altimetry map[13]. This geophysical dataset allows
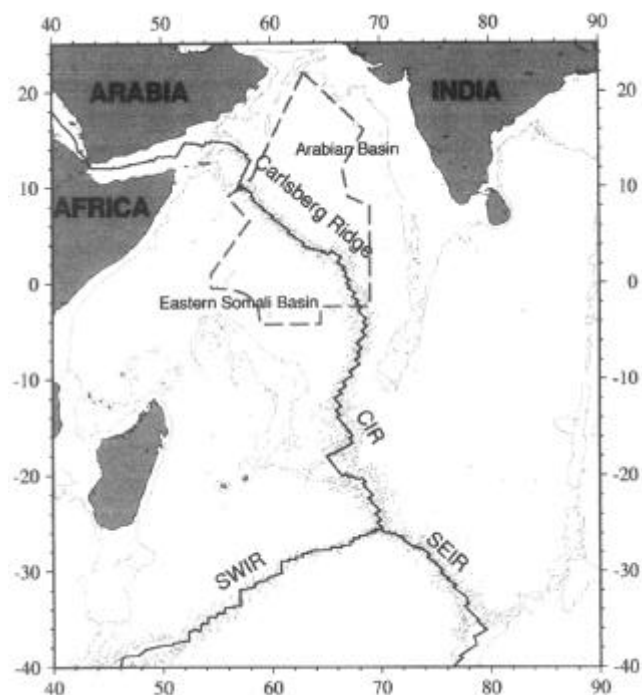

Figure 1. Generalized map of the northwest Indian Ocean. The Central Indian and Madagascar basins are conjugate basins as flanks of CIR (Central Indian Ridge) and Arabia and Somalia basins as flanks of Carlsberg Ridge. The full dashed line encloses the area where marine magnetic anomaly profiles were obtained. Bathymetric contours at 3000 m and were taken from ETOPO5 map[23].

*For correspondence. (e-mail: SAM@ns1480.spb.edu)

studying of almost 1300 km along ridge section and more than 10 Ma across the ridge. In addition to our dataset, we have extracted the data from NGDC[14] files to study the early evolution of the proto-CR during the Palaeocene–Eocene period.

Results and discussion

The magnetic anomaly map of the CR and Eastern Somali and Arabian basins (Figure 2) depicts two discordant systems of linear magnetic anomalies. One corresponds with fast spreading with respect to latitudinal axis of the proto-ridge, and the other corresponds to slow spreading with respect to modern axis of the CR. The main feature of the two spreading systems is the asymmetry relative to each other and relative to axial anomaly.

The analysis of magnetic anomaly and bathymetric data (Figure 3) shows the clear limit between the roughness of the bathymetry and the regularity of the abyssal hills in the Eastern Somali basin (0.5°N, 60°E) to the NW. The position of the similar limit in the Arabian basin was obtained by reconstruction. These linear structures observed in the magnetic field and bathymetry suggest that the spreading geometry of the Proto-CR has changed in the form of propagating rift from Southeast to Northwest during anomaly time 24–20.

The studied part of CR has a complex structure and is characterized by an en-echelon system of spreading centres. The comprehensive analysis of the magnetic and bathymetric data reveals transform/non-transform discontinuities (Figure 4). The observed variation in spreading direction of the ridge subdivides the region in two distinct parts on either side of 2.5°N–66°E. The northwestern part is characterized by a general trend almost orthogonal to the present spreading direction, while the southeastern one has about 45° oblique trend compared to the spreading direction. We have defined segments as well-individualized bathymetric high and MBA (Mantle Bouger Anomaly) low. The axis of CR is segmented into 26 accretion segments (10–85 km length) separated by two major 100–150 km long transforms and several 2nd–4th-order discontinuities with offsets of 30 km or no offsets. Along the northwestern ridge section, the axis is made up of 20 segments (mean length of 50 km). Most of the discontinuities have small or zero offsets, only two of them are transform faults. Along the southeastern section, the ridge consists of six segments separated by larger offset (up to 100 km) discontinuities, among which some are not transform faults but oblique relays.

The bathymetric and MBA variation along axis (Figures 4 and 5) also show two different sections, the limit of which is at (3.5°N–64°E) more than 200 km west of the 'geometric' limit, discussed above. The southeastern part is characterized by along axis MBA variations of smaller
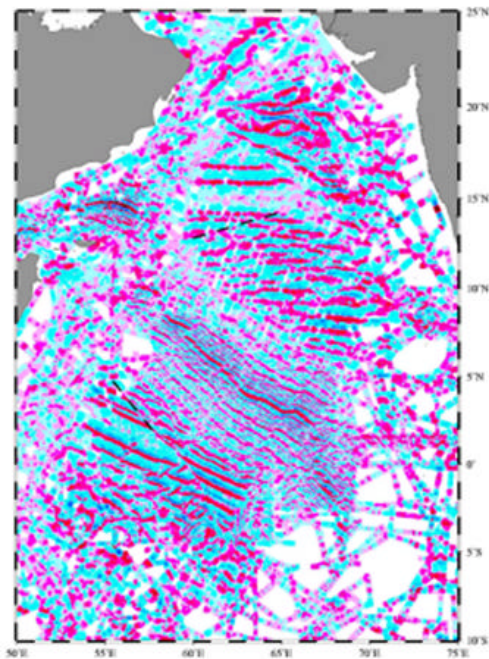

Figure 2. Colour-scale image of magnetic anomalies in the NW Indian Ocean. Dashed lines correspond to pseudofaults of Carlsberg Proto Ridge during westward propagating rift (see also Figure 3).
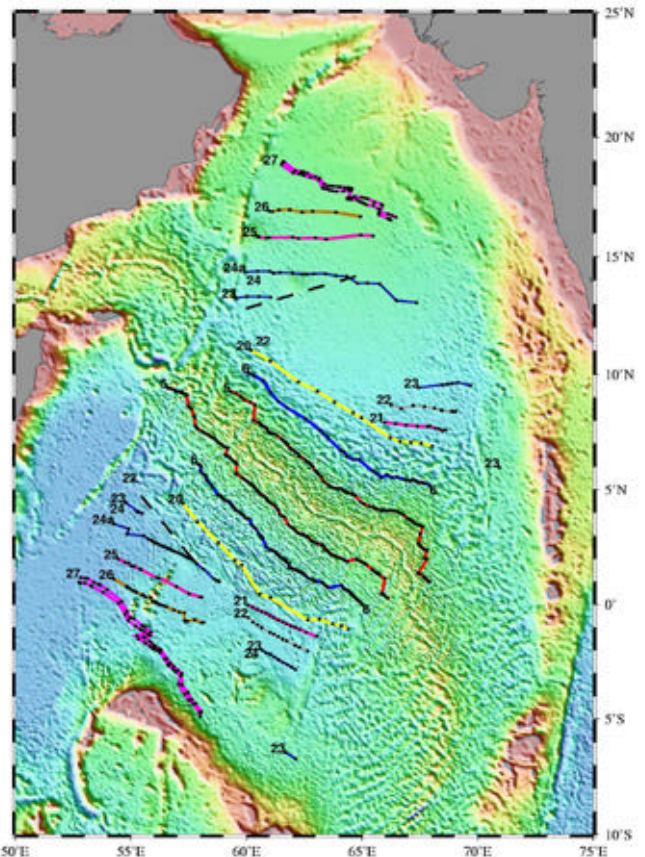

Figure 3. Shaded bathymetric map of the NW Indian Ocean with magnetic lineation. Russian dataset grided at 2 min spacing is merged with predicted bathymetry[14].

amplitude with a mean axial MBA value being more negative than along the northwestern part.

The ridge axis geometry, which is inherited from the opening of the oceanic basins, appears to control the morphology of the ridge, but do not control the deep structure, as the MBA values suggest a more continuous magmatic source beneath these chaotic morphology. This difference in deep structure could be due to a combination of hot-spot influence and increasing spreading rate southward. The analysis of axial magnetic anomalies, spreading rate and direction confirm that the ridge segmentation is not the adaptation of inherited plate boundary geometry to changes in spreading conditions but the effect of the accreting processes, focused magma upwelling along discrete spots of the slow spreading axis. The segment scale morphological variations and associated axial MBA suggest along-axis variations in the magmatic and tectonic processes.

Full sequences of magnetic anomalies up to A5 (10 Ma) have been identified on the CR by generating synthetics for each profile (Figures 6 and 7). The mean half-spreading rate increases from 1.2 cm/yr to 1.5 cm/yr from NW to SE. The spreading rate for the west and east flanks of CR and the spreading rate distribution for anomaly A5 along the CR (Figure 6) have been computed using A5-CR finite rotation pole (24.2°N, 28.3°E). The synthetic model has been computed by Tisseau and Patriat method[16], using magnetic reversal scale of Candy and Kent[16,17] taking magnetized layer thickness of 1 km at depth increasing

Figure 5. Mantle Bouguer anomaly over the Carlsberg Ridge. Gravity dataset is obtained from the global FAA deduced from satellite altimetry map[13]. Thick black line represents the axis of ridge segments.
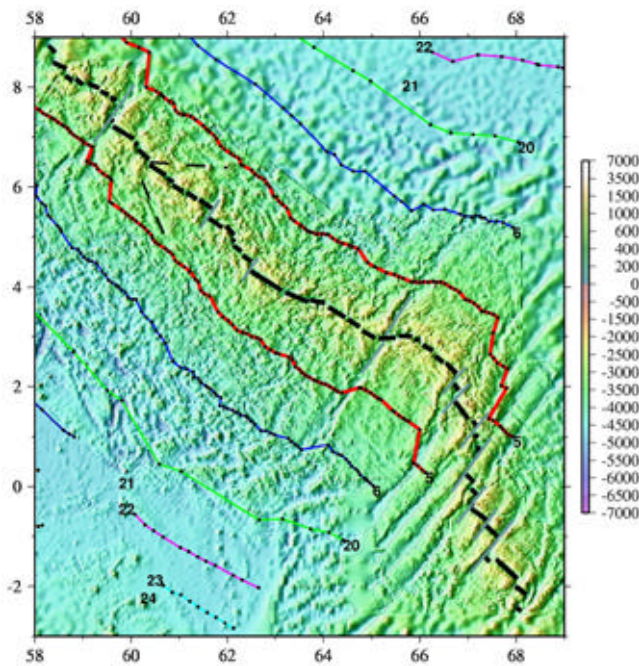

Figure 4. Shaded bathymetric map over Carlsberg Ridge with magnetic lineation, transform faults (grey plain line) and axis ridge segments (thick black line). Magnetic picks are plotted as points and magnetic lineation are plotted as colour lines and numbered; dashed light lines are traces of ridge propagation.
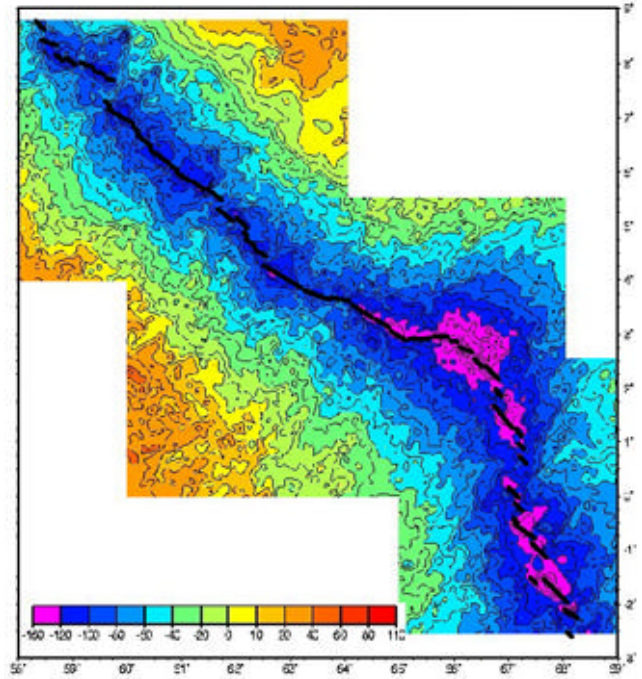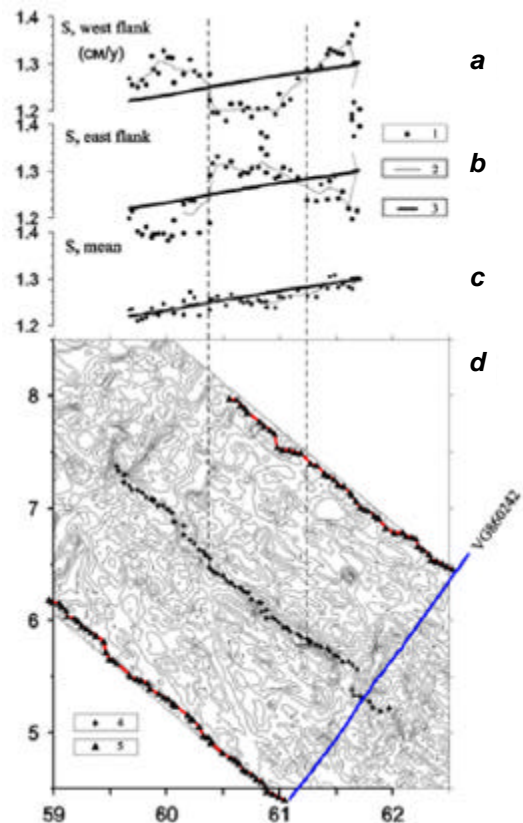

Figure 6. Spreading rate distribution for anomaly A5 along Carlsberg Ridge. 1, Spreading rate obtained for the west (**a**) and east (**b**) flanks of CR and half-full spreading rate (**c**), 2, Running average; 3, Theoretical half-full spreading rate calculated using A5-CR pole finite rotation (24.2 N; 28.3 E); 4, Carlsberg spreading axis; 5, Magnetic pick of anomaly 5.
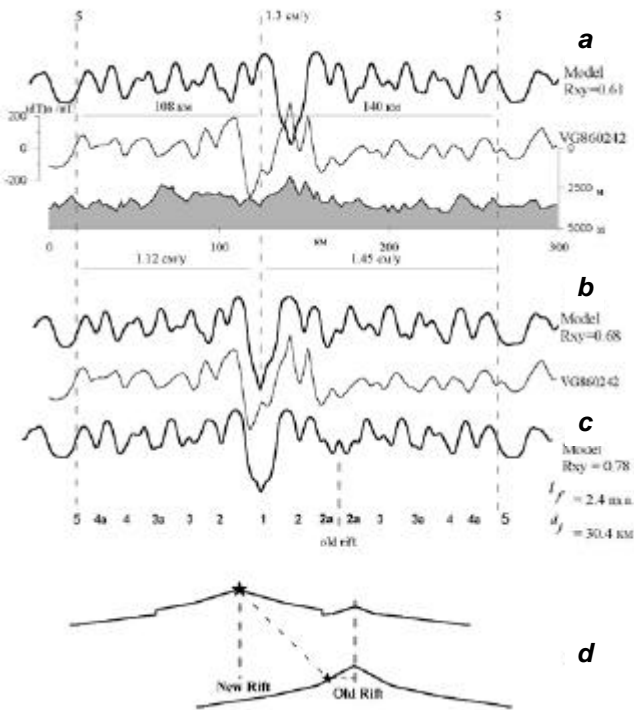
Figure 7. Possible identifications of the magnetic anomalies observed on the CR (profile VG860242, see location on Figure 6) according to either a symmetrical (*a*) or an asymmetrical (*b* and *c*) spreading model. *d*, Sketch showing jumping spreading ridge.

with age[18] and the magnetization intensity adjusted for matching the synthetic and observed amplitudes (Figure 7). The asymmetrical model (Figure 7 *c*) is the best fitting model with ridge jump at a distance of 30.4 km on west flank of the CR, 2.5 m.y. ago, which matches with the observed profile VG860242 and gives high correlation ($R = 0.78$).

The intra- and inter-segmental variation in spreading rate has been studied. The distribution of average spreading rate for the last 10 Ma is not always symmetric. The observed asymmetry is not attached to one flank or one period but seems rather randomly distributed resulting into the continuously changing offsets. This asymmetry is the result of either inter-segment axis jump or intra-segment propagation[19,20].

We have used the principle of ordering (ranking)[21] for building of the lithological correlation for magnetic anomaly identification and jumping ridge-axis location. This principle consists in affirmation that a curve joining the correlation points is a monotone function. The correlation points are those where the highest coefficient of correlation between an interval on one curve and all intervals of the same length on other curve is obtained. The basic idea of the algorithm used is the combination of the ordering principle and similarity measure. Using this technique of maximum cross-correlation of similar aligned features, we have located the time and distance of the ridge jump. The symmetrical model (Figure 8, top) shows
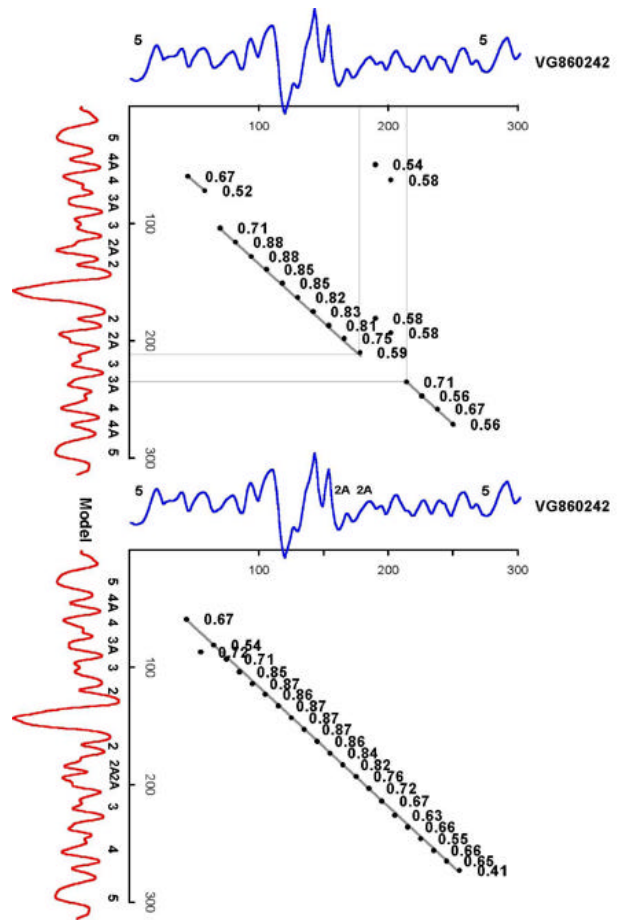

Figure 8. Objective of the magnetic anomalies identification by the correlation figures method applied to the observed and calculated profiles of Figure 5. Each solid circle with its associated number is related to a short section of the observed profile and indicates the location along the model where the best value of correlation is obtained.

the low correlation between anomalies 2A and 3A, whereas the asymmetrical model with axis ridge jump provided good correlation. The best correlation (Figure 8, bottom) was obtained after comparison between observed profile and more than 200 models calculated by varying various arguments of a spreading ridge jump. Thus, we find that the method of maximum cross-correlation of similar aligned fragments and resulting correlation figures determine the best time and distance of the ridge jump. The identification of magnetic anomalies allows determining isochrones on both flanks. However, the superposition of two conjugate isochrones is not accurate. A variable slope of the block limits coming from the 3-D ridge structure could explain this misfit.

Conclusion

We find that prior to the Himalayan collision, seafloor spreading on the Carlsberg proto-ridge was extremely active. A major reorganization of the spreading plate

boundaries in the Indian Ocean during Eocene, as a consequence of the hard collision of India with Eurasia, led to the slow spreading on the present CR. Our results show that during both these periods the structure and spreading on the CR was non-stationary.

1. Wiseman, J. D. H., Scientific Reports of the John Murrar Expedition, Britizh Museum, Natural History, 1937, vol. 3, pp. 1–28.
2. Drolia, R. K., Indian Ocean Ridge System (IORS): Results update, challenges and opportunities in the new millennium, National workshop on 'Trends in ocean sciences – 21st century' at Regional Center, National Institute of Oceanography, Visakhapatnam, September 2000, pp. 28–30.
3. Fournier, M., Patriat Ph. and Leroy, S., Reappraisal of the Arabia–India–Somalia triple junction kinematics. *Earth Planet. Sci. Lett.*, 2001, **189**, 103–114.
4. Bernard, A., Le bassin des Mascareignes et l'arc des Amirants, temoins de l'uverture au Cretace de l'ocean Indien occidental: apport de la geophysique. Ph D thesis, Univ. de Strasbourg, 1998, pp. 1–276.
5. Matthews, D. H., Vine, F. J. and Cann, J. R., Geology of an area of the Carlsberg Ridge. *Geol. Soc. Am. Bull.*, 1965, **76**, 675–682.
6. McKenzie, D. P. and Sclater, J. G., The evolution of the Indian Ocean since the late Cretaceous. *Geophys. J.*, 1971, **24**, 437–528.
7. Todal, A. and Edholm, O., Continental margin off Western India and Deccan large igneous province. *Mar. Geophys. Res.*, 1998, **20**, 273–291.
8. Mercuriev, S., Patriat, Ph. and Sochevanova, N., Evolution de la dorsale de Carlsberg: Evidence pour une phase d'expansion tres lent entre 40 et 25 Ma (A18 a A7). *Oceanol. Acta*, 1996, **19**, 1–13.
9. Ramana, M. V., Ramprasad, T., Kamesh Raju, K. A. and Desa, M., Geophysical studies over a segment of the Carlsberg ridge, Indian Ocean. *Mar. Geol.*, 1993, **115**, 21–28.
10. Kameh Raju, K. A., Kodagali, V. N. and Fujimoto, H., Three dimensional gravity and magnetic studies over a segment of the Carlsberg Ridge, Indian Ocean. 35th Annual Convention of Indian Geophysical Union held at National Institute of Oceanography, Goa, December 1998, pp. 29–30.
11. Mudholkar, A., Kamesh Raju, K. A., Kodagali, V. N., Afzulpurkar, S. and Ambre, N. V., Exploration of the Carlsberg Ridge. *InterRidge News*, 2000, **9**, 32–33.
12. Mudholkar, A. V., Kodagali, V. N., Kamesh Raju, K. A., Valsangkar, A. B., Ranade, G. H. and Ambre, N. V., Geomorphological and petrological observations along a segment of slow-spreading Carlsberg Ridge. *Curr. Sci.*, 2002, **82**, 982–989.
13. Sandwell, D. T. and Smith, W. H. F., Marine gravity anomaly from Geosat and ERS 1 satellite altimetry. *J. Geophys. Res.*, 1997, **102**, No. B5, 10039–10054.
14. Tisseau, I. and Patriat, Ph., Identification des anomalies magnetiques sur les dorsales a faible taux d'expansion: methode des taux fictifs. *Earth Planet. Sci. Lett.*, 1981, **52**, N2, 381–396.
15. Cande, S. C. and Kent, D. V., Revised calibration of the geomagnetic polarity timescale for the late Cretaceous and cenozoic. *J. Geophys. Res.*, 1995, **100**, 6093–6095.
16. Cande, S. C. and Kent, D. V., A new geomagnetic polarity time scale for the late Cretaceous and Cenozoic. *J. Geophys. Res.*, 1992, **97**, N.B10, 13917–13951.
17. Parsons, B. and Sclater, J. G., An analysis of the variation of ocean floor bathymetry and heat flow with age. *J. Geophys. Res.*, 1977, **82**, 803–827.
18. Merkouriev, S., Rommevaux-Jestin, C., Patriat, Ph. and Sotchevanova, N., Large scale segmentation of a 1300 km long section of the Carlsberg Ridge from bathymetry, gravimetry and magnetism. Eos Trans. AGU Fall Meeting November 16, 1999, **80**, N 46, F1049.
19. Merkouriev, S. and Sochevanova, N., Asymmetry of magnetic anomalies and model of jumping spreading axis on an example of Carlsberg Ridge. in Materials of the 27th session of an International seminar by Uspensky, Moscow, 2000, pp. 122–123.
20. Jekhowsky, B., La methode des distances minimales, nouveau procede quantitatif de correlation stratigraphique; example d'application en paleontologie. *Rev. Inst. Franc. Petrole, Paris*, 1963, **18**, N5, 629–653.
21. Wessel, P. and Smith, W. H. F., Free software helps map and display data, EOS. *Trans. Am. Geophys. Union*, 1991, **72**, 445–446.
22. ETOPO5 Relief map of the Earth's surface. *EOS Trans. AGU*, 1986, **67**, 121.
23. NGDC/MGG-National Geophysical Data Center for Marine Geology and *G*eophysics. *Bolder*, 2002.